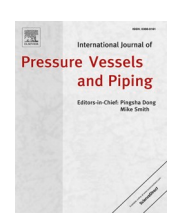
FISEVIER

Contents lists available at ScienceDirect

# International Journal of Pressure Vessels and Piping

journal homepage: www.elsevier.com/locate/ijpvp





# A comprehensive comparison of creep-fatigue life assessment through leading industrial codes

Younes Belrhiti <sup>a,\*</sup>, Cory Hamelin <sup>b</sup>, Pierre Lamagnère <sup>c</sup>, David Knowles <sup>a,d</sup>, Mahmoud Mostafavi <sup>e</sup>

- <sup>a</sup> Department of Mechanical Engineering, University of Bristol, Bristol, BS8 1TR, UK
- <sup>b</sup> UK Atomic Energy Authority, Culham Science Centre, Abingdon, Oxfordshire, OX14 3DB, UK
- CEA DES/IRESNE/DTN/STCP, CEA Cadarache, 13108, Saint Paul-Lez-Durance, France
- <sup>d</sup> Henry Royce Institute, Manchester, M12 9PL, UK
- <sup>e</sup> Department of Mechanical and Aerospace Engineering, Monash University, Clayton, Victoria, 3800, Australia

#### ABSTRACT

Creep-fatigue damage has been recognized as a critical failure mode for high-temperature structures. In fusion power reactors, plasma-facing components endure complex loading conditions, resulting in high thermomechanical stresses. These components, often made from 316L material, joined to ferritic-martensitic steels, face significant challenges due to the interaction of various loads affecting their material properties and structural integrity. This paper compares internationally recognized methods for creep-fatigue assessment: the R5 procedure and the RCC-MRx code.

The study evaluates the differences and similarities in creep-fatigue assessments between these procedures, providing a global overview and a detailed comparison. The conservatism of both approaches are assessed by comparing the material properties dataset, total strain calculations, and lifetime estimates for 316L at 550 °C. Additionally, the welding assessment approaches of RCC-MRx and R5 are compared and applied to similar metal welds (316L-to-316L). Further, dissimilar Electron Beam Welded metals (316L-to-10CrMo9-10) are prepared, investigated and characterized using creep-fatigue experiments to compare the predicted service life using RCC-MRx.

#### 1. Introduction

Creep-fatigue damage has been recognized as a significant and potentially life-limiting failure mode for high-temperature structures since the middle of the 1960s [1]. Initially identified by the nuclear sector, its significance gained momentum with apprehensions regarding aerodynamic heating in aircraft and hypersonic flights [2]. Additionally, creep-fatigue damage became a concern in the petrochemical, natural gas, and fossil power generation industries [3], as their facilities began to operate at increasingly higher temperatures and respond to fluctuating loads on the electrical grid, leading to failures attributed to creep-fatigue interaction [4].

In fusion power reactors, plasma-facing components endure challenging and multifaceted loading conditions, encompassing major thermal variations, electromagnetic loads including disruption events, pressure loads arising from cooling channel water, convective heat loads, and irradiation [5]. Consequently, they face exceptionally high thermomechanical (steady-state and cyclic) stresses. Several components in a fusion power reactor (e.g. the vacuum vessel) will be made from 316L material and, in cases like DEMOnstration fusion reactor

(DEMO), these structures are expected to be joined to ferritic-martensitic steels (e.g. where breeding blanket structures are joined to the vacuum vessel). There are currently knowledge gaps regarding the interaction of various loads on components, and how these interactions impact the performance and structural integrity of the components [6]. Among these interactions, creep-fatigue assessment remains a key parameter in predicting the service life of the components.

Fatigue damage is typically, but not exclusively, defined as the initiation of a transgranular crack associated with a persistent slip band impinging on a grain boundary. In contrast, creep damage is generally an intergranular mechanism occurring at grain boundaries and associated with the nucleation, cavitation, and coalescence of cavities and voids [7]. This makes creep damage a distributed mechanism, occurring simultaneously at many locations in the material, whereas fatigue damage nucleates only at a few critical locations. The interaction of creep and fatigue, therefore, is not attributed to a single mechanism and depends on various parameters such as the material's properties, temperature, and type of loading [8,9].

To ensure a safe and reliable design, high-temperature design codes and procedures have evolved, incorporating years of experience in assessing the lifetime integrity of specific components. A crucial element

E-mail address: younes.belrhiti@gmail.com (Y. Belrhiti).

 $<sup>^{\</sup>ast}$  Corresponding author.

$\begin{array}{c} \overline{\varepsilon}, \overline{\Delta\varepsilon} \\ \overline{\sigma}, \overline{\Delta\sigma} \\ \overline{\delta\varepsilon_1} \\ \overline{\Delta\varepsilon_2} \\ \overline{\Delta\varepsilon_3} \\ \overline{\Delta\varepsilon_4} \\ \overline{\Delta\varepsilon_{fl}} \\ \Delta\overline{\varepsilon_{pol}} \\ \end{array}$ $\begin{array}{c} \varepsilon_L \\ d_f \\ E \\ \varepsilon_S \\ \overline{E} \end{array}$	Equivalent strain, equivalent strain range Equivalent stress, equivalent stress range Strain range given by elastic analysis Plastic strain due to the primary stress range Plastic enhancement from the elastic stress Plastic increase from triaxiality Strain amplification due to creep per cycle Correction to strain range due to change to constant volume deformation in plasticity Lower shelf ductility Fatigue damage per cycle Young's Modulus Secant modulus Effective elastic modulus in R5: Factor applied to S., to obtain material ratchet limit.	$n_{j}$ $N_{j}$ $P$ $P_{b}$ $P_{L}$ $P_{m}$ $F$ $Q$ $S'_{y}$ $S_{m}$ $S_{y}$ $\sigma_{ref}^{R}$ $U$ $V$ $W$ $v$ $\Delta \overline{\sigma}_{el,r}$	Number of applied cycles of type $j$ Allowable number of cycles of type $j$ Primary stress Bending stress Local membrane stress Membrane stress Peak stress Secondary stress Creep modified yield stress (R5) Allowable stress(RCC-MRx) The minimum monotonic 0.2 % proof stress The rupture reference stress (R5) Creep usage factor due to primary loads (R5) Fatigue usage factor Creep usage rupture factor(RCC-MRx) Poisson ratio Equivalent stress range adjusted by $\Delta \sigma_{rD}$
$egin{array}{c} \overline{E} \ K_s \ K_ u \end{array}$	Effective elastic modulus in R5: Factor applied to $S_y$ to obtain material ratchet limit, in RCC-MRx: symmetrisation coefficient Amplification coefficient (RCC-MRx)		

in these rules is the inclusion of a creep-fatigue assessment, mandated for nuclear installations and fusion reactors, in cases where creep-fatigue is assumed to occur. For a prototypic fusion power reactor, it is assumed that primary fatigue damage is caused by the pulsed operation of the fusion reactor while creep damage occurs during operation at elevated temperatures. In the presence of creep, the fatigue life of a component is reduced.

This paper compares internationally recognized methods for determining creep-fatigue initiation endurance: the R5 procedure [10] and the RCC-MRx code [11]. The detailed analysis highlights key similarities and differences in their assessment methodologies. The "Assessment Procedure for the High Temperature Response of Structures" known as the R5 procedure, has undergone a 45-year evolution within the UK nuclear industry. Developed by the Central Electricity Generation Board (CEGB) and now owned by EDF Energy Nuclear Generation Limited, these procedures are crucial for assessing Nuclear Power Plant component integrity at both high and low temperatures, considering creep-induced material degradation. They encompass the evaluation of defect-free structures, as addressed in design codes, and defect tolerance. The R5 assessment procedures are used internationally and the R5 Volume 2/3 crack initiation procedure is instrumental in demonstrating the integrity of nuclear safety-significant components operating at high temperatures, including those with the highest reliability.

RCC-MRx is a design code used for high-temperature reactors, fusion reactors, and research reactors. It outlines regulations encompassing material specifications, design criteria, fabrication processes, examination procedures, installation protocols, testing requirements, marking standards, and report preparation for components operating in conditions involving significant creep and/or irradiation. Originally formulated in 1983 based on insights from French fast sodium reactors (Phenix and Superphenix), the code was subsequently expanded in 2007 to include fusion applications (ITER Vacuum vessel) and in 2012 for research reactors (Jules Horowitz reactor). RCC-MRx, a pivotal reference code, has been instrumental in projects such as the Astrid project (Advanced Sodium Technological Reactor for Industrial Demonstration) in France, irradiation devices for the Jules Horowitz reactor in France, the primary circuit of MYRRHA (Multipurpose Hybrid Research Reactor for High-tech Applications) in Belgium, and the target of the European Spallation Source in Sweden.

The present work aims to evaluate the differences in creep-fatigue assessments between these procedures, acknowledging their inherent similarities but also identifying potentially substantive variations. The

structure of this paper is organized to provide a global overview of the creep-fatigue life assessment using the R5 procedure and the RCC-MRx code, highlighting their main similarities and differences. Then, a detailed comparison is followed by an analysis of 316L material properties under identical conditions in both procedures and the impact of the variation of some material parameters on the assessment. The comparison between the procedures is, then, evaluated by comparing both total strain calculations and lifetime estimates that are obtained using each procedure, for 316L at 550  $^{\circ}\mathrm{C}$ .

Following this, the RCC-MRx and R5 welding assessment approach is compared and applied to similar metal welds (316L-to-316L). Additionally, dissimilar metal weldments (DMW) 316L-to-10CrMo9-10 were prepared using the Electron Beam Welding (EBW) technique. The microstructure is investigated and creep-fatigue experiments are conducted on these samples and compared to the predicted service life obtained using RCC-MRx.

#### 2. Materials and methods

#### 2.1. Creep-fatigue life assessment procedures

A generic procedure for some creep-fatigue assessment procedures [10,12,13] is illustrated in Fig. 1. The first step involves evaluating the external loads and thermal conditions that the component withstands during service life and describing the cyclic conditions. Using material properties and elastic finite element (FE) simulation, critical stress/strain locations are identified for creep-fatigue assessment. These locations are determined based on the elastic total stress range and maximum temperature during the cycle. The simplest approach to determine the stress/strain condition is based on the post-processing of the FE simulation output, by considering the calculated stress and total strain (elastic, plastic, and creep) [14]. If data is unavailable, creep-fatigue tests are conducted under conditions similar to the identified critical locations to assess the damage summation diagram and determine criteria for creep-fatigue interaction in the studied alloy. The crack initiation locus in a creep-fatigue damage summation diagram should be validated through tests simulating the real cycle at the critical location. Although expensive, these benchmark tests are essential for validating the entire creep-fatigue damage assessment procedure.

Fig. 1. Generic flow diagram representing the analysis process adopted by many defect-free creep-fatigue assessment procedures.

#### 2.2. Creep-fatigue interaction assessment in R5 vs. RCC-MRx

In this paper, the creep-fatigue interaction approaches of R5 [10] and RCC-MRx [11] are used and compared. The R5 approach selected here is detailed in Volume 2/3: creep-fatigue crack initiation procedure for defect-free structures [10]. The RCC-MRx 2018 edition assessment applied here is detailed in Figure RB 3216a [11] corresponding to level A analysis criteria and negligible irradiation. The 2018 edition is not the latest one and modifications in creep-fatigue design rules have been implemented in the 2022 edition.

# 2.2.1. High-level comparison

In this section, an overview of the main observations from comparing the two approaches is presented. Table 1 summarizes the main similarities and differences between them. These points will be discussed in detail in the sections following Table 1 [15].

# 2.2.2. Analysis approach and stress classification

R5 and RCC-MRx apply the same general approach to general stress classification, where the stresses are split into.

- primary stresses P (Pm, Pb, and PL),
- secondary stresses Q, and
- · peak stresses F.

# 2.2.3. Plastic collapse and stress limits

The approaches to protect against plastic collapse are generally similar but not identical in RCC-MRx (P damage prevention rules) and R5 for load-controlled stresses. The approaches consider basic design limits for  $P_m$  and  $P_L + P_b$  to a prescribed stress threshold defined as:

$$P_m \le X \tag{1}$$

$$P_L + P_b \le 1.5X \tag{2}$$

where X is:

- $\bullet$  The allowable stress  $S_m$  in RCC-MRx (RB 3251.11 [11]).
- $\frac{2}{3}S_y'$  in R5 [10]. For austenitic and ferritic steels, the creep-modified yield stress  $S_y' = S_y$ .  $S_y$  is the minimum monotonic 0.2 % proof stress.

In the negligible irradiation and significant creep condition, type P

damage prevention rules in RCC-MRx propose additional requirements, as detailed in RB 3252.11 [11]. R5 provides the following checks against plastic collapse or excessive plastic deformation when including the secondary equivalent stress against the total stress range:

$$\Delta(P_L + P_b + Q) \le 2S_v \tag{3}$$

$$\Delta(P_L + P_b + Q) \le 2.7S_v \tag{4}$$

(3) is for ferritic steels and (4) for austenitic stainless steels.

RCC-MRx applies checks on the applied loads to prevent progressive deformation from cyclic loads (S damage) as:

$$\max(P_L + P_h) + \Delta Q \le 3S_m \tag{5}$$

This equation applies only in the case of negligible creep. An efficiency diagram can be used to prevent progressive deformation in negligible or significant creep [16].

# 2.2.4. Creep fatigue assessment

The general approach in RCC-MRx and R5 to calculate the fatigue usage factor (with different terminology) is given by:

$$V = \sum_{i} \left( \frac{n_{i}}{N_{j}} \right) \tag{6}$$

where:

- $n_i$  is the number of applied cycles of type j
- *N<sub>j</sub>* is the allowable number of cycles (of type *j*) and is calculated using the determined total strain range.

In RCC-MRx, the total strain range used in the fatigue assessment (RB 3261.1123) is calculated in the case of significant creep as follows:

$$\overline{\Delta\varepsilon} = \overline{\Delta\varepsilon_1} + \overline{\Delta\varepsilon_2} + \overline{\Delta\varepsilon_3} + \overline{\Delta\varepsilon_4} + \overline{\Delta\varepsilon_f}$$
 (7)

where:

•  $\overline{\Delta \varepsilon_1}$  is the strain range given by elastic analysis,

$$\overline{\Delta\varepsilon_1} = \frac{2}{3} (1 + \nu) \cdot \left( \frac{\overline{\Delta\sigma_{tot}}}{E} \right) \tag{8}$$

Table 1
R5 and RCC-MRx creep-fatigue interaction global approaches comparison.

		Similarities	Differences
Analysis approach	h	R5 and RCC-MRx use the same general approach to stress classification (primary, secondary and peak stresses).  The approaches to protect against plastic collapse are generally similar but not identical.	The stress limits for P damage prevention rules and against progressive deformation (S damage) are not the same.
Creep-fatigue assessment	Fatigue approach	<ul> <li>Strain range calculation:</li> <li>The elastic term in R5 corresponds to Δε<sub>1</sub> in RCC-MRx.</li> <li>The plastic term in R5 to Δε<sub>3</sub> in RCC-MRx.</li> <li>The volumetric strain Δε<sub>νο1</sub> in R5 is similar to Δε<sub>4</sub> in RCC-MRx but with K<sub>ν</sub> calculated directly.</li> <li>Both approaches use Neuber construction for the elastic-plastic strain.</li> <li>Both approaches use the fatigue usage factor definition (with different terminology) and fatigue curves.</li> </ul>	In the strain range calculation, there is not an equivalent term to $\overline{\Delta e_2}$ (RCC-MRx) in R5. R5 proposes two methods for strain calculation (simplified and detailed). In R5, the calculation of the fatigue damage $d_f$ per cycle is related to crack nucleation and can be adjusted to account for the initiation of a defect of a given size, whereas the RCC-MRx use the endurance curves defined from a specific load drop which can correspond to a relatively large crack size and include margins calculated from the average fatigue curve.
	Creep approach	To estimate creep rupture time or creep endurance, the minimum creep rupture stress curves are used in RCC-MRx and R5.	<ul> <li>R5 uses a ductility exhaustion approach to assess creep damage, whereas RCC-MRx uses a time-fraction approach:</li> <li>In RCC-MRx, creep strain uses creep laws which consider creep time.</li> <li>In R5, stress relaxation data is used for creep strain calculation. In RCC-MRx stress relaxation can be taken into account using creep strain rates</li> <li>The definition of the stress used as input to the creep rupture curves differs between the approaches of the two codes even if the basic approaches are quite similar.</li> <li>In RCC-MRx, the creep usage rupture factor W is used and is different from d<sub>c</sub> creep damage used in R5.</li> </ul>
	Interaction diagram	The use of a creep-fatigue interaction diagram for the determination of the allowable cycle before failure. If the assessment point falls within the envelope, the crack initiation is avoided. If the point falls on or outside the envelope, then crack initiation is predicted.	The interaction diagram in RCC-MRx uses the fatigue usage fraction $V$ and the creep usage fraction $W$ , and the one used in R5 is coupling fatigue damage $d_f$ and creep damage $d_c$ .
	Weld assessment	The weld assessment is based on the parent metal assessment after applying specific factors.  There is a correspondence between weld types:  • Type 1 in R5 corresponds to I.1, I.2, I.3, II.1 in RCC-MRx  • Type 2 in R5 corresponds to III.1, III.2 in RCC-MRx  • Type 3 in R5 corresponds to V, VI, and VII in RCC-MRx	In R5, the strain range is multiplied by a weld strain enhancement factor ( <i>WSEF</i> ). It is not necessary to multiply the portion of the cycle that includes the dwell by the <i>WSEF</i> . Creep dwell stress is enhanced before calculating the creep strain but the <i>WSEF</i> is then only multiplied by the plastic strain range and volumetric strain. The R5 assessment includes the effects of residual stresses for an initial calculation of some relaxation damage which is not normally significant and the impact of the weld geometry (weld cap angle, dressed or undressed weld). In RCC-MRx, stress calculation depends on the welding type (full or partial penetration). For P and S damage checks and creep-fatigue interaction, the assessment is done by multiplying the limits and parent curve by factors ( $n$ , $J_f$ , $J_b$ , $f$ ) which depend on the weld type and the examination applied.
Material data		Each code has its exclusive database from which the data should be used: R66 for R5, and the appendixes of RCC-MRx	There are some differences in material properties in R66 and RCC-MRx for the same materials at the same conditions that can influence the conservatism of the approach



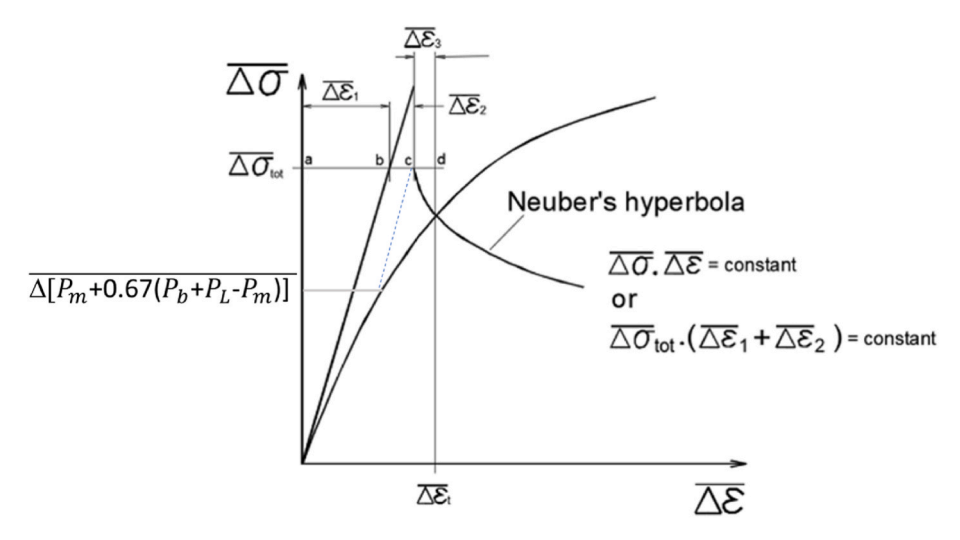


Fig. 2. Graphical description of how to determine  $\overline{\Delta \varepsilon_2}$  and  $\overline{\Delta \varepsilon_3}$  using the cyclic curve (from Ref. [6]).

•  $\overline{\Delta \varepsilon_2}$  is the plastic increase in strain due to the primary stress range at the point under examination and is calculated along the path "b-c" shown in Fig. 2. The point "c" is determined, as shown in Fig. 2, using the stress:

$$\overline{\Delta\sigma} = \overline{\Delta[P_m + 0.67(P_b + P_L - P_m)]} \tag{10}$$

 $\overline{\Delta \varepsilon_2}$  is generally very low compared to  $\overline{\Delta \varepsilon_1}$  and can be practically ignored [6].

- $\overline{\Delta \varepsilon_3}$  represents the plasticity enhancement from the initial elastic stress. This follows a Neuber construction where  $\overline{\Delta \sigma}.\overline{\Delta \varepsilon}$  is constant, allowing the analyst to move from a point given by  $(\overline{\Delta \varepsilon_1} + \overline{\Delta \varepsilon_2}, \overline{\Delta \sigma_{el}})$  to the intersection with the cyclic stress-strain curve. The additional strain is defined along path "c-d" as  $\overline{\Delta \varepsilon_3}$ , as shown in Fig. 2 and in Figure RB 3261.1123 in Ref. [11]. A less conservative evaluation of  $\overline{\Delta \varepsilon_3}$  not shown here can be used in the case of pure secondary stress (peak thermal stress, for example).
- $\overline{\Delta \varepsilon_4}$  provides the plastic increase from triaxiality. This is given by:

$$\overline{\Delta\varepsilon_4} = (K_p - 1)\overline{\Delta\varepsilon_1} \tag{11}$$

where  $K_{\nu}$  is provided from look-up tables [11] for specific temperature and stress range.

•  $\overline{\Delta \varepsilon_{fl}}$  is the additional creep strain over each cycle in cases where creep is deemed significant. The strain is dependent on the elastic-plastic stress range. The strain amplification due to creep per cycle is calculated using the creep law given in A3.54 [11] and a specific stress  $\sigma_k$  detailed below.

To calculate N, the allowable number of cycles or the number of cycles to failure, the value of  $\overline{\Delta \varepsilon}$  is used with the fatigue curves given in A3.47 [11].

In R5, different methods can be used to estimate the total strain used for creep-fatigue assessment.

# - Simplified method [10]

This method is used if creep effects can be neglected or when the creep dwell starts at the hysteresis loop tip (C in Fig. 3) and the elastic follow-up is assumed to be moderate (Z < 5).

The total strain range  $\Delta \overline{\varepsilon}_t$  is obtained as follows:

$$\Delta \overline{\varepsilon}_t = \left[ \frac{\Delta \overline{\sigma}}{\overline{E}} + \left( \frac{\Delta \overline{\sigma}}{A} \right)^{1/\beta} \right] + \Delta \overline{\varepsilon}_{vol}$$
 (12)

where:

- $\overline{E} = 3E/2(1 + \nu)$
- $\bullet$  The total strain range  $\Delta \overline{\epsilon}$  is obtained by solving

$$\Delta \overline{\sigma}_{el,r} \Delta \overline{\varepsilon}_{el,r} = \frac{\left(\Delta \overline{\sigma}_{el} + \Delta \sigma_{rD}\right)^{2}}{\overline{E}} = \Delta \overline{\sigma} \left[ \frac{\Delta \overline{\sigma}}{\overline{E}} + \left(\frac{\Delta \overline{\sigma}}{A}\right)^{1/\beta} \right]$$
(13)

$$\Delta \,\overline{\sigma} = \Delta \overline{\sigma}_{\rm el} + \Delta \overline{\sigma}_{\rm rD} \tag{14}$$

$$\Delta \overline{\varepsilon}_{el,r} = \Delta \overline{\sigma}_{el,r} / \overline{E} \tag{15}$$

 $\Delta \sigma_{rD}$  is the stress drop under constant strain creep relaxation.

•  $\Delta \bar{\epsilon}_{vol}$  is the enhancement due to the constant volume deformation which occurs during plastic strain and estimated from:

$$\Delta \overline{\varepsilon}_{vol} = (K_{\nu} - 1) \Delta \overline{\varepsilon}_{el,r} \tag{16}$$

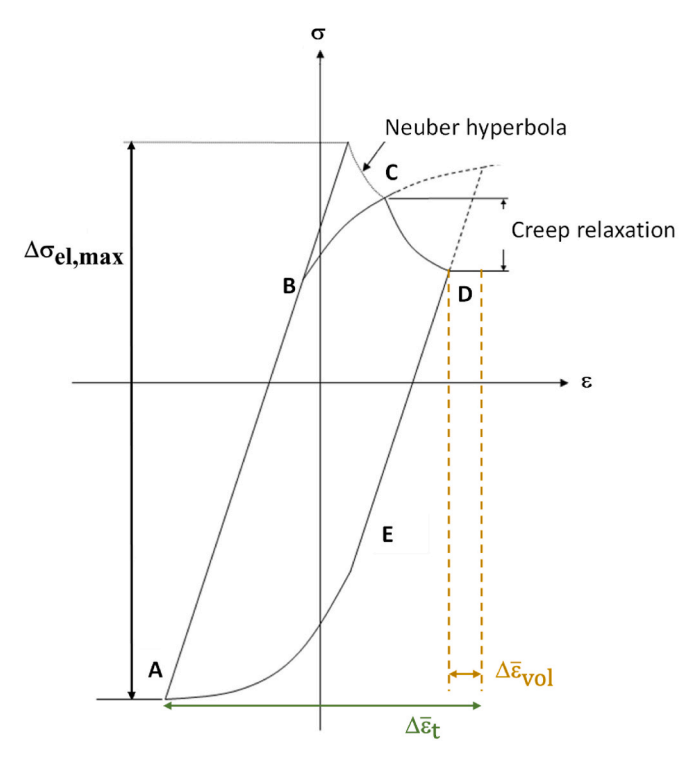


**Fig. 3.** Schematic of simple hysteresis curve with creep relaxation (from Ref. [10]).

$$K_{\nu} = \left(\frac{1+\overline{\nu}}{1+\nu}\right) \left(\frac{1-\nu}{1-\overline{\nu}}\right) \tag{17}$$

$$\overline{\nu} = \nu \frac{E_s}{\overline{E}} + 0.5 \left( 1 - \frac{E_s}{\overline{E}} \right) \tag{18}$$

$$E_{\rm s} = \frac{\Delta \overline{\sigma}}{\left[\Delta \overline{\sigma} / \overline{E} + (\Delta \overline{\sigma} / A)^{1/\beta}\right]} \tag{19}$$

- Detailed method for the enhancement of strain range in the presence of creep

This method (detailed in Appendix 07 [10]) is based on the construction of the adjusted hysteresis material cyclic curve, starting with the construction of the half cycle not including creep for the off-peak dwell cycle (ABC in Fig. 3). Construction details are given in A7.5.3 [10].

The loop positioning on the stress axis is carried out using the  $K_sS_y$  limits primarily to define  $\sigma_D$ . The stress range for this half-cycle corresponding to the stress at the start of creep is then calculated by solving:

$$\frac{\left(\Delta \overline{\sigma}_{el,a}\right)^{2}}{\overline{E}} - (\sigma_{N} + \sigma_{D}) \left(\frac{\sigma_{N} + \sigma_{D}}{\overline{E}} + \left(\frac{\sigma_{N}}{A^{*}}\right)^{\frac{1}{\beta}}\right) = 0 \quad \textit{for} \quad \Delta \overline{\sigma}_{el,a} \geq \sigma_{D} \quad (20)$$

where:

- $\sigma_N$  is the stress at the intersection between the Neuber construction curve and the appropriate half-cycle representation of the stress-strain range relationship.
- A\* is a modified Ramberg-Osgood parameter
- $\beta$  is the Ramberg-Osgood parameter  $\beta$  for the cyclic material curve
- $\Delta \overline{\sigma}_{el,a}$  is the adjusted elastic stress range.
- $\overline{E}$  is the modified Young's modulus  $\overline{E} = 3E/(2(1 + \nu))$

 σ<sub>D</sub> is the datum stress, a stress offset. The value of this stress varies depending on the curve being used. Its value is defined for each construction phase in the A7.5.3 [10].

The drop in stress  $\Delta \sigma_{rD}$  (CD in Fig. 3) is estimated from suitable relaxation data, available in material property handbooks such as R66 [17]. The total strain range  $\Delta \bar{\epsilon}_t$  is then calculated from the sum of the greatest half-cycle strain range and its corresponding volumetric strain enhancement  $\Delta \bar{\epsilon}_{vol}$ :

$$\Delta \overline{\varepsilon}_{vol} = (K_{\nu} - 1) \Delta \overline{\varepsilon}_{el} \tag{21}$$

In R5 fatigue assessment, the fatigue damage per cycle  $d_f$  corresponding to the cyclic strain range  $\Delta \bar{\epsilon}_t$  is defined as:

$$d_f = \frac{1}{N_0} \tag{22}$$

where:

 N<sub>0</sub> is the number of cycles to initiate a crack of size a<sub>0</sub> under continuous cycling conditions at strain range Δē<sub>t</sub>.

$$N_0 = N_i + N_\sigma \tag{23}$$

• N<sub>i</sub> corresponds to the number of cycles for crack nucleation

$$ln(N_i) = ln(N_{\ell}) - 8.06N_{\ell}^{-0.28} \tag{24}$$

- $N_{\ell}$  is determined using the endurance data available in material property handbooks [17] and the total strain range  $\Delta \bar{\epsilon}_t$
- N'g corresponds to the number of cycles for crack growth, which is not considered in this paper.

In RCC-MRx, the creep usage rupture factor  $\boldsymbol{W}$  is calculated using the following equation:

$$W = \sum_{k} \left(\frac{t_k}{T_k}\right) \tag{25}$$

where:

- $t_k$  is the creep time of cycle type k
- $T_k$  is the allowable time for that condition to cause creep rupture using the creep rupture curves  $S_r$  with an enhanced stress level  $\frac{\sigma_k}{\Omega\Omega}$ .
- $\sigma_k$  is calculated as detailed in RB 3262.1123 [11].

$$\sigma_k = \overline{P}_{max} + K_s.\overline{\Delta S^*}$$
 (26)

 $\bullet$   $\overline{P}_{max}$  is the maximum value of the equivalent primary stress during the temperature maintenance time

$$\overline{P}_{max} = Max[\overline{P_m + 0.66(P_b + P_L - P_m)}]$$
(27)

- $K_s$  in RCC-MRx corresponds to the symmetrisation coefficient obtained using the curve A3.46 [11] and is different from  $K_s$  used in R5 which is applied to Sy to obtain material ratchet limit.
- $\overline{\Delta S^*}$  is the variation of the secondary stress (RB 3262.1123b in Ref. [11])
- relaxation of the secondary stress during the holding time can be taken into account using creep strain rate deduced from creep strain laws

Using the minimum creep rupture stress curves  $S_r$  given in A3.53 [11], it is possible to determine the creep rupture time at a  $S_r$  value equal to  $\frac{\sigma_k}{\Omega \cdot \Omega}$ . In RCC-MRx, the fatigue usage fraction  $V(\overline{\Delta \varepsilon})$  and the creep

rupture usage fraction  $W(\sigma)$  are used in conjunction with the creep–fatigue diagram given in A3.55 [11] (Fig. 4a) to determine the number of cycles to failure in the presence of creep.

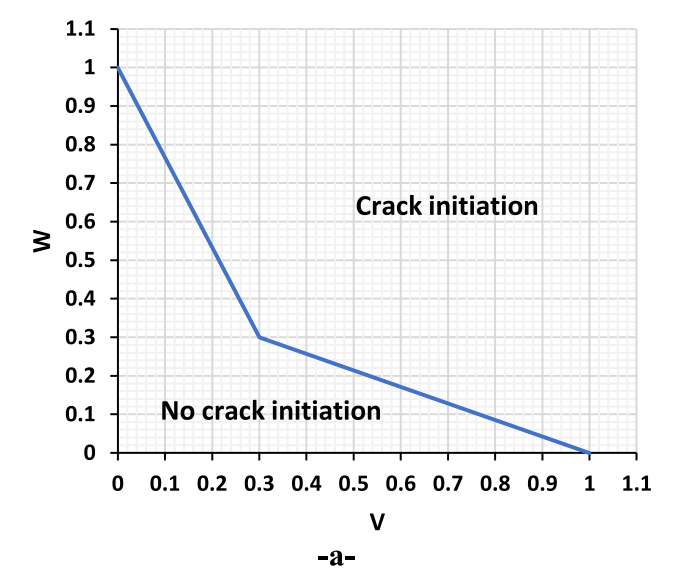
A distinguishing feature of the R5 method is that it adopts a ductility exhaustion approach to assess creep damage rather than a time fraction approach as in other codes [18]. The creep damage per cycle  $d_c$  is therefore given by:

$$d_{c} = \int\limits_{\overline{e}_{f}(factors \ affecting \ ductility)}^{t_{h}} dt \tag{28}$$

where:

- $\bullet$   $\dot{\bar{c}}_c$  is the instantaneous equivalent creep strain rate during the dwell period
- $\overline{\varepsilon}_f$  is the appropriate creep ductility
- t<sub>h</sub> is the duration of the creep dwell

For the case involving a tensile dwell where it is assumed that the most onerous stress state during the dwell period applies at all times and



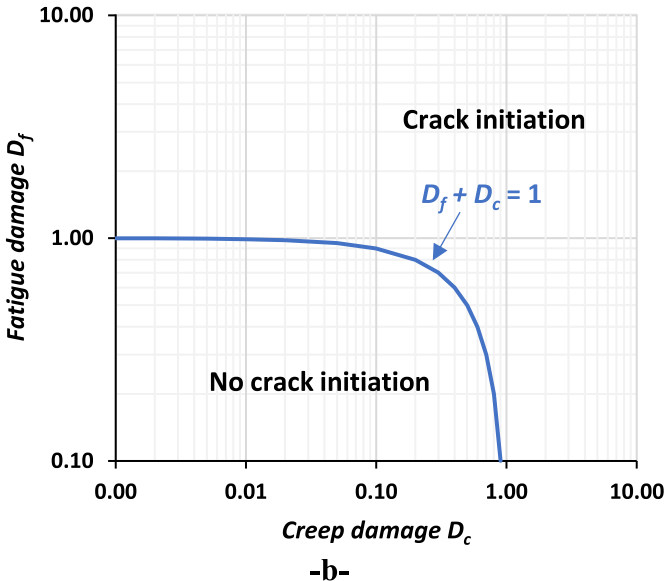


Fig. 4. Creep-fatigue interaction diagram for 316L in RCC-MRx (-a-) and the damage curve in R5 (-b-).

that the creep ductility is independent of stress and strain rate and equal to the lower shelf ductility  $\varepsilon_L$  suitably factored to take into account of stress state  $(\overline{\varepsilon}_L)$ , the creep damage per cycle is given by:

$$d_c = \frac{Z\Delta\overline{\sigma}}{\overline{E}_{F_c}} \tag{29}$$

where:

- Z is the elastic follow-up factor
- $\Delta \overline{\sigma}'$  is the equivalent stress drop allowing for elastic follow-up

The creep strain is then obtained using the following equation:

$$\Delta \varepsilon_c = \frac{Z\Delta \sigma_{rD}}{\overline{E}} \tag{30}$$

The total creep-fatigue damage D for the loading history is found by linear summation of the fatigue and creep damage increments for each cycle type:

$$D = D_f + D_c \tag{31}$$

where:

$$D_f = \sum_{j} \frac{n_j}{N_{0j}} = \sum_{j} n_j d_{jj}$$
 (32)

$$D_c = \sum_i n_j d_{cj} \tag{33}$$

 $n_j$  is the number of service cycles of type j and  $N_{oj}$ ,  $d_{fj}$  and  $d_{cj}$  are the values of  $N_0$ ,  $d_f$  and  $d_c$  corresponding to that cycle type. The parameters  $D_f$  and  $D_c$  are used to define the Damage diagram (Fig. 4b).

If the assessment point  $(D_c, D_f)$  falls within the envelope (D < 1), then crack initiation is avoided. If the point falls on or outside the envelope (D > 1), then crack initiation is predicted.

# 2.2.5. Weld treatment

Historically, weldments have been analyzed in R5 as the parent material; the difference in the behaviour of the weldment compared to the parent material is addressed using a Fatigue Strength Reduction Factor (FSRF). The FSRF considers reductions in fatigue endurance and enhancements in strain due to material mismatch and local geometry effects. Two separate assessment routes are provided for weldments in the undressed (as-welded) and dressed conditions. In both instances,

FSRFs are used to enhance the strain range, reducing the endurance of the weldment in both cases. For dressed welds peak (F) elastic stresses are used to evaluate the start of dwell stress values. For undressed welds, linearized stresses are employed and the FSRF-modified strain is utilized to determine the start of dwell stress.

It was generally recognized that the approach above is overly pessimistic, and rather than incorporate geometrical and material effects, the new modified approach, which is described in detail in Fig. 5, separates the two effects.

The procedure corresponding to metal weldments is described in Appendix A4 [10]. This appendix provides a procedure for the assessment of austenitic and ferritic steel weldments based on Fig. 5, but including a modification to the approach used to account for stress concentration effects. The calculation of creep-fatigue damage is covered in Section 8 and Figure A4.4 [10].

It applies to dressed and undressed weldments and utilizes a single assessment route for both types of weldments.

The new approach in R5 separates the existing FSRF into the following components [10,18].

- a Weld Strain Enhancement Factor (WSEF), which accounts for strain enhancement due to the weldment geometry (if applicable) and the material mismatch between weldment zones.
- a Weld Endurance Reduction (WER), which accounts for the fatigue endurance reduction due to the presence of small imperfections (e.g. inclusions, porosity etc.)

Further, the modified procedures have been simplified by adopting a single route both for dressed and undressed weldments through the use of linearized stresses.

Firstly, the applicable elastic strain range is determined. If an undressed weld is being considered the local stress range is enhanced by a Stress Concentration Factor (*SCF*). It should be applied to the linearized stress:

$$SCF = \lambda \left(\frac{\theta}{30}\right)^{0.5} \tag{34}$$

where  $\theta$  is the weld cap angle in degrees,  $\lambda$  is taken as 1.15 for undressed welds and 1 for dressed welds.

The WSEF is applied to the plastic strain range including volumetric correction  $\Delta \bar{\epsilon}_{t1}$ . Then, adding the increase in creep strain during the dwell  $\Delta \bar{\epsilon}_{t2}$ :

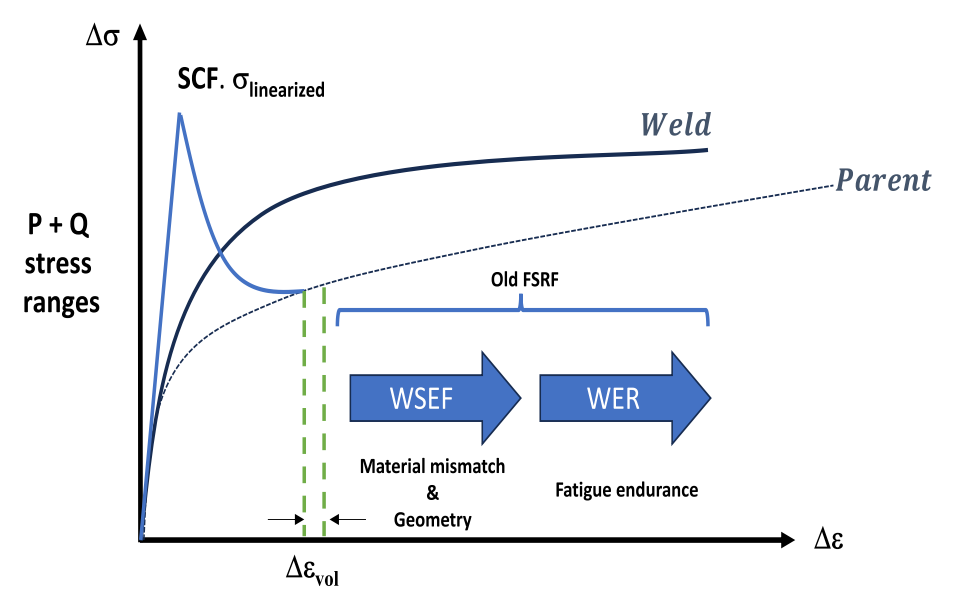


Fig. 5. Schematic of the modified route showing the split of FSRF into WSEF and WER.

$$\Delta \overline{\varepsilon}_t = WSEF. \Delta \overline{\varepsilon}_{t1} + \Delta \overline{\varepsilon}_c \tag{35}$$

The resulting strain range  $\Delta \bar{\epsilon}_t$  is then used to calculate the fatigue damage, which is calculated using either the reduced parent material fatigue endurance curve (i.e. reduced by the *WER*) or the weld metal fatigue endurance curve, whichever is lower. So, both the *WER* and *WSEF* are used in the calculation of fatigue damage.

 $\it WSEF$  values depend on the R5 Weld Type and the parent material as described in Table 2.

Weld assessment conducted using RCC-MRx is based on the calculation of structure behaviour without considering the mechanical properties of welds. Then, specific factors are applied for the assessment.

The stress calculation in the weld depends on the welding type: full penetration (RB 3293.1 in Ref. [11]) or partial (RB 3293.2 [11]). In the case of full penetration, the stresses are calculated as if the two assembled parts formed a single continuous piece without any welding.

To check the compliance with rules preventing P damage, the rules are the same as presented in  $\S 1.2.3$  however,  $S_m$  is replaced by  $n.J_m.S_m$  where:

- *n* is the weld coefficient, which depends on the type of joining and control type (Table RB 3291.1 in Ref. [11]).
- $J_m$  is the welding characteristic coefficient (table A9 in Ref. [11]).

Fatigue and creep assessment of the weld approach (S damage prevention) is similar to that presented above, with the following differences.

- A reduction factor f to the calculated stress to consider local stress concentrations inside the weld or on the surface. The value of f depends on the type of weld and controlling technique (Table RB 3292.112 in Ref. [11]).
- The fatigue weld reduction factor  $J_f$  is applied to fatigue curves of the parent in cases where fatigue curves of the weld (A9 in Ref. [11]) are not available.
- The allowable stresses  $S_r$  of the parent is replaced by  $n.J_r.S_r$ .

In the case of dissimilar welds, the properties of the weakest joined materials are selected for the weld assessment.

#### 3. Results and discussion

#### 3.1. Materials properties comparison

A comparison of material properties of 316L [19] versus temperature used in the R5 assessment (based on data in R66 [17]) and those used in the RCC-MRx assessment (based on data in Appendix A3.3Sin that code) were made

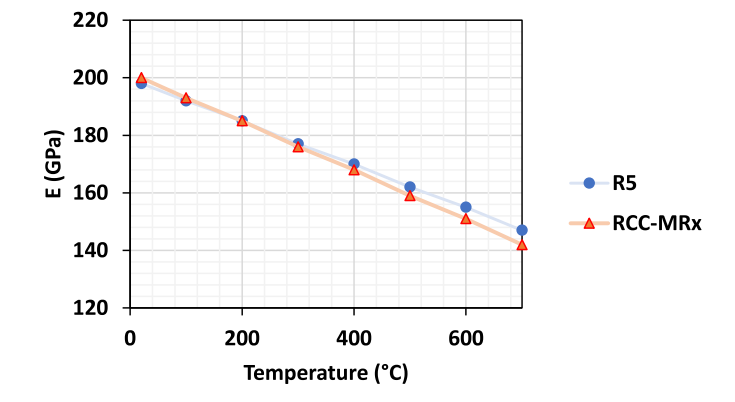
It was noticed for 316L that there were significant differences in some material properties for specific temperatures.

Fig. 6a and Fig. 6b compare respectively Young's modulus and minimum values of  $R_{p0.2}$  % of 316L versus the temperature defined by the two codes. The values are almost the same up to 300  $^{\circ}\text{C}.$  Beyond this temperature, the values proposed by the RCC-MRx become more conservative than those used in R5.

It is worth mentioning that the tensile properties have undergone

**Table 2**WSEF values depending on weld type and the parent material.

R5 Weld	RCC-MRx corresponding type	WSEF		
type		Austenitic weldments	Ferritic weldments	
1	I.1, I.2, I.3, II.1	1.16	1.5	
2	III.1, III.2	1.23	2.5	
3	V, VI, VII	1.66	3.2	



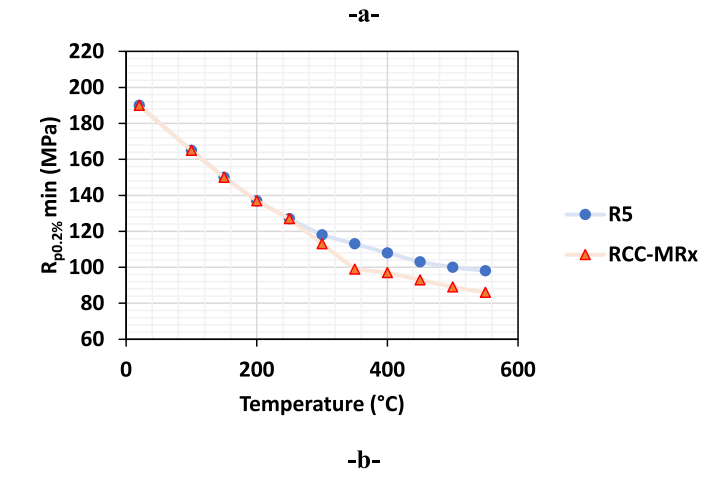


Fig. 6. 316L Young modulus (-a-) and minimum values of  $R_{\rm p0.2~\%}$  (-b-) vs temperature.

revision since the edition of R66 [17] used in this comparison. Fig. 7a and Fig. 7b compares the thermal properties (thermal conductivity and thermal expansion coefficient respectively) of 316L defined by the two codes. In the case of thermal properties, RCC-MRx provides higher, and so more conservative, values than R5 for 316L as a higher thermal expansion coefficient will induce higher thermal stresses [20].

Fig. 8 compares cyclic curves for 316L provided at 550  $^{\circ}\text{C}$  by the two codes, RCC-MRx values are more conservative.

Fig. 9 compares the lower bound allowable fatigue curves for 316L provided by the two codes at  $550\,^{\circ}\text{C}$ . RCC-MRx provides fatigue design curves including safety margins resulting in more conservative values than those available and used in R5. In addition to the safety margins, these differences can be related to the differences in testing conditions, chemical compositions, manufacturing process and heat treatment conditions.

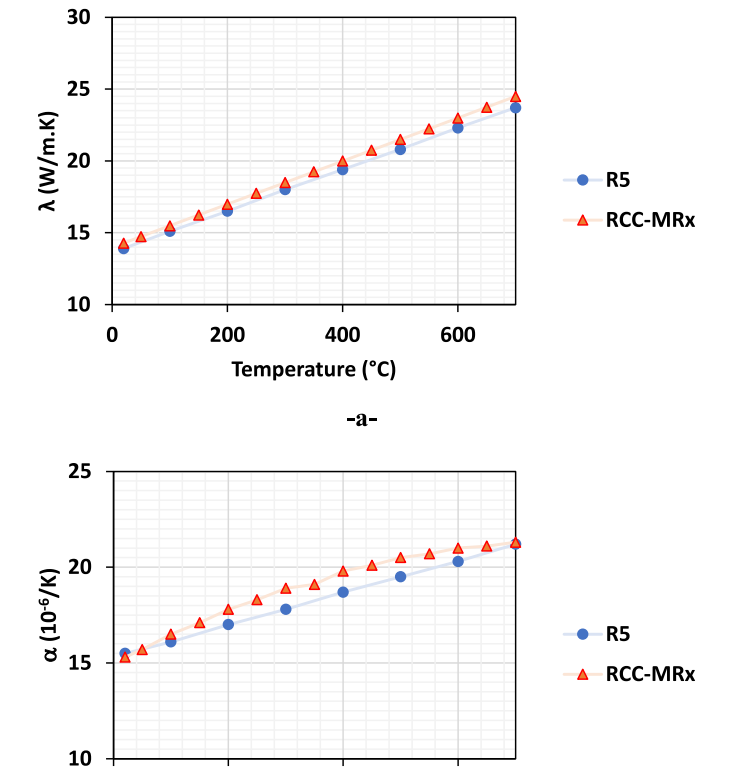
Fig. 10 compares the lower bound allowable creep rupture stress versus corresponding creep hours at 550 °C provided by the two codes. The comparison of the data shows that the available values used in R5 are more conservative than those in RCC-MRx for the same value of creep rupture stress. It is worth mentioning that the stress used as input to the creep rupture curves differs between the approaches as explained above. The reference stress used in step 5 of R5 [10] (creep endurance satisfactory) seems to be lower than  $\sigma_k$  used in the calculation of the creep usage factor of RCC-MRx [21].

#### 3.2. Strain calculation comparison

The strain calculation approaches used in RCC-MRx and R5 (simplified and detailed) presented in  $\S1.2.4$  were used to calculate elastic, elastic-plastic, volumetric, and total strains for 316L at 550 °C. A

0

200



**-b- Fig. 7.** 316L thermal conductivity (-a-) and instantaneous thermal expansion coefficient (-b-) vs temperature.

400

Temperature (°C)

600

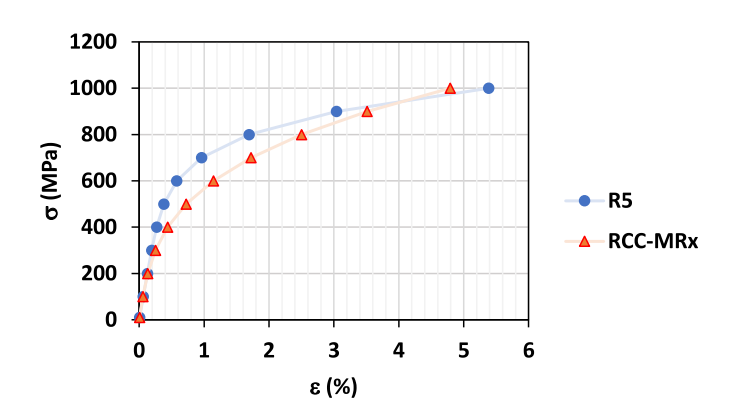


Fig. 8. 316L stress vs strain cyclic curves at 550  $^{\circ}\text{C}.$ 

total stress range of 400 MPa and a dwell time of 300 h were selected.  $P_m$  and  $P_L+P_b$  values selected are the maximum values satisfying Eq. (1) and Eq. (2).

The approach to calculating the strain range that is input to the creep-fatigue assessment does differ between the two codes however there are many similarities.

The elastic term in R5 in Eq. (12) corresponds to  $\overline{\Delta \varepsilon_1}$  in RCC-MRx (§1.2.4), the plastic term to  $\overline{\Delta \varepsilon_3}$  and the volumetric strain  $\overline{\Delta \varepsilon_{vol}}$  is similar to  $\overline{\Delta \varepsilon_4}$  but with  $K_{\nu}$  calculated directly. There is not an equivalent term to  $\overline{\Delta \varepsilon_2}$  in R5 as this considers a mean plastic enhancement from primary loads which is typically very small. If there is no variation in primary loads,  $\overline{\Delta \varepsilon_2}$  is equal to zero in RCC-MRx in agreement with R5.

Fig. 11 represents a comparison between the calculated strains using

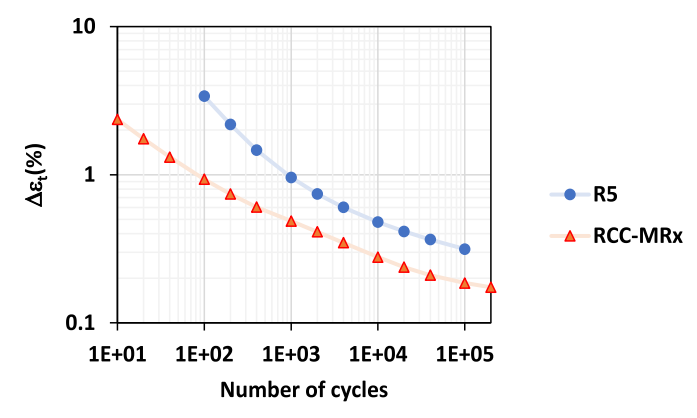


Fig. 9. 316L lower bound allowable fatigue strain range values vs numbers of fatigue cycles at 550  $^{\circ}\text{C}.$ 

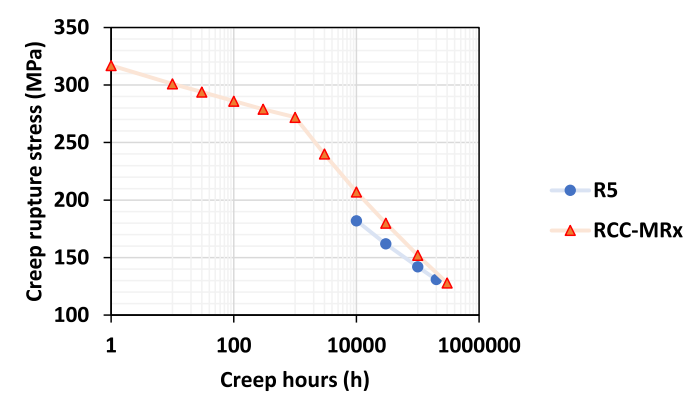


Fig. 10. 316L lower bound allowable creep rupture stress range values vs creep hours at 550  $^{\circ}\text{C}.$ 

RCC-MRx and R5 (simplified and detailed approaches).

The R5 simplified method results in larger estimates of plastic strain range than the detailed route which leads to accurate prediction of stress levels. These differences are negligible in the present load case. The total strain calculated using RCC-MRx for 316L at 550  $^{\circ}\text{C}$  under 400 MPa stress load is higher than the one estimated using R5, and so, RCC-MRx is more conservative.

# 3.3. Influence of material data variation on the assessment

It is worth mentioning that material data used in the R5 calculation are from R66 and differ from those used in RCC-MRx at  $550\,^{\circ}$ C. And so,

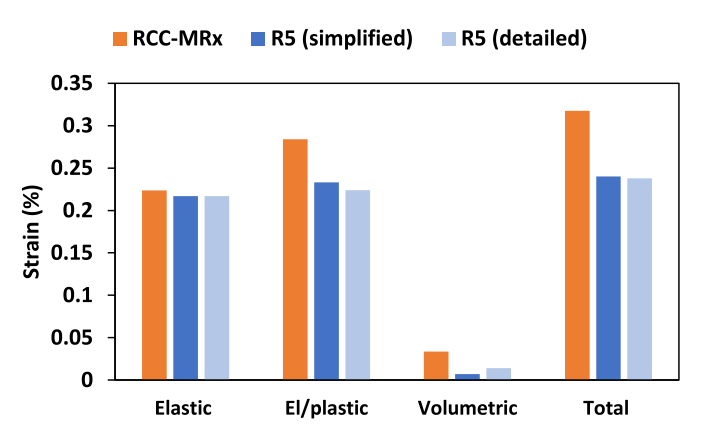


Fig. 11. 316L strain calculation comparison at 550  $^{\circ}\text{C}$  between RCC-MRx and R5.

the differences between the strain values are related to the differences in the assessment approaches in addition to the material properties (§2.2). Indeed, when we use the R66 material data (E,  $\nu$ , the cyclic curve) of 316L at 550 °C in the RCC-MRx assessment, the elastic and plastic strains calculated using the RCC-MRx procedure are quite similar to the one evaluated using R5 detailed analysis as shown in Fig. 12.  $K_{\nu}$  value used for calculating  $\Delta \varepsilon_4$  in Eq. (11) remains unmodified (from A3.3S.463 [11]), as the derivative equation for  $K_{\nu}$  values tabulated in A3.3S.463 (RCC-MRx) differs from that in Eq. (17) of the R5 assessment. The total strain doesn't include the creep strain here.

The most significant source of variation between the two codes in calculating total strain is the material properties. By switching material properties, elastic and plastic strain values are quite similar, and their contribution to total strain calculation is significant. The second source of variation is the volumetric strain, due to differences in  $K_{\nu}$  calculation between the codes. The values given in RCC-MRx ( $K_{\nu}=1.15$  in A3.3S.463 [11]) are higher than those calculated in R5 ( $K_{\nu}=1.031$  for the simplified method and  $K_{\nu}=1.062$  for the detailed method).

Besides, to conduct an assessment, various parameters specific to the material, temperature and mechanical stress are used. These parameters require careful consideration, as they directly impact the assessment. For example, the influence of the variation of the  $K_{\nu}$  factor on the assessment has been investigated.

 $K_{\nu}$  values are provided in look-up tables for specific temperatures and stress ranges [11], and vary between 1.12 and 1.17 for 316L. Fig. 13a shows strains calculated using three different values of  $K_{\nu}$ , the total strain calculated here includes the creep strain. This figure illustrates the impact of  $K_{\nu}$  on the calculation of allowable fatigue cycles (Fig. 13b). The variation in  $K_{\nu}$  can result in a difference of  $\pm$  80 cycles in the assessment.

#### 3.4. Creep-fatigue life prediction

# 3.4.1. Study case 1: 316L

To assess creep-fatigue interaction for 316L at 550  $^{\circ}$ C under a total stress range of 400 MPa and a dwell time of 300 h, creep strain is calculated and added to the total strain.

- $\overline{\Delta \varepsilon_{fl}}$  used in RCC-MRx is calculated thanks to the creep law given in A3.54 [11].  $\overline{\Delta \varepsilon_{fl}}$  (%) = 0.36. Stress relaxation using creep strain rates was not considered here.
- $\overline{\Delta\varepsilon_c}$  used in R5 is calculated using the stress drop  $\Delta\sigma_{rD},~Z=1$  and  $\overline{E}$  (A11 of [10]).  $\overline{\Delta\varepsilon_c}$  (%) = 0.008

R5 uses creep ductility ( $\varepsilon_L=9$  %), where RCC-MRx uses a time-fraction approach and so the latter is likely to calculate greater creep damage over a set time period despite having a lower average stress drop.

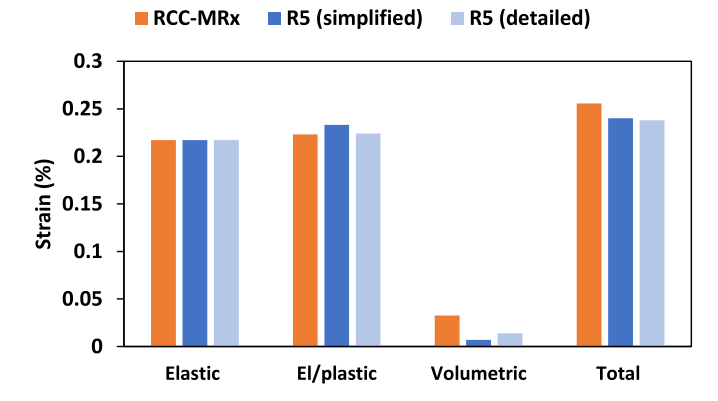


Fig. 12. 316L strain calculation comparison at 550  $^{\circ}\text{C}$  between RCC-MRx (using R66 data) and R5.

In R5, fatigue and creep damage per cycle,  $d_f$  and  $d_c$  respectively, are calculated using equations (22), (29) and (31).

- $d_f = 2.76E-05$
- $d_c = 9.40$ E-04
- $D = d_f + d_c = 0.000968$

Considering Fig. 4b corresponding to the crack initiation envelope, the allowable creep-fatigue cycles before crack initiation are predicted in Table 3. In RCC-MRx, using fatigue curves (Table A3.3S.47 in Ref. [11]) and the total strain including the creep strain, the allowable fatigue cycles are 999 cycles. Using creep curves (Table A3.3S.53a in Ref. [11]), the allowable creep hours are 2977 h leading to a creep usage fraction  $W(\sigma)$ =0.1.

From the 316L creep fatigue diagram (Fig. 4a), the allowable creepfatigue cycles before rupture with a dwell time of 300 h are predicted in Table 3.

In addition to the more conservative aspects of strains calculated using RCC-MRx in comparison with R5, the difference between the allowable creep-fatigue cycles obtained using the two codes can be justified by the following.

- the approach in R5 considered here is related to crack nucleation and can be adjusted to account for the initiation of a defect of a given size, whereas the RCC-MRx use the endurance curves defined from a specific load drop (which can correspond to a relatively large crack size) and so RCC-MRx allows fewer cycles.
- the differences in material properties and the rupture curves used (Fig. 9) between the two codes also have an impact on the results.
- the treatment of creep and fatigue damage in R5 and RCC-MRx are not similar. R5 considers a linear addition of the two damage values, whereas, RCC-MRx uses an interaction between creep strain and fatigue damage.

#### 3.4.2. Study case 2: 316L similar metal weld

Creep-fatigue assessment of welded 316L samples (full penetration, Type I.1) at  $550^{\circ}$ C under a total stress range of 400 MPa and a dwell time of 300 h was performed using R5 and RCC-MRx.

The RCC-MRx assessment is performed after applying.

- ullet a reduction factor f=1 from Table RB 3292.112 in Ref. [11] (considering a weld type I.1 and volume control or surface examination during welding). This factor is applied to the stress value. As the welding is full penetration the stress calculation is done as if the two assembled parts formed a single continuous piece.
- a fatigue weld reduction factor  $J_f = 1.25$  is applied to the fatigue curves of the parent 316L. The fatigue curve of 316L (Fig. 9) was used after applying  $J_f$ .
- the allowable stresses S<sub>r</sub> of the weld S<sub>rjs</sub> for 316L parent are given in table A9.J3S.53 in Ref. [11].

Using the creep-fatigue interaction diagram of 316L (Fig. 4a), the allowable creep-fatigue cycles are  $106\ \text{cycles}$ .

R5 weld assessment is conducted as described in  $\S 1.2.5.$ 

- *WSEF* = 1.16 (type I weld)
- the selected weld is a dressed weld ( $\lambda=1$ ) without a weld cap ( $\theta=0$ ) and so the SCF defined in Eq. (34) is not considered here.

Table 3 Allowable creep-fatigue cycles calculated using R5 and RCC-MRx approaches at 550  $^{\circ}\mathrm{C}$ 

	R5	RCC-MRx
316L	1033	750
316L-316L	782	106

- The enhanced strain corresponding to the plastic and volumetric strain is  $\Delta \bar{\epsilon}_{f1}$  (%) = 0.24
- Creep strain increment per cycle is estimated using Eq. (30) (considering Z = 1)  $\Delta \bar{\epsilon}_c$  (%) = 0.007
- And so, the fatigue strain range  $\Delta \overline{\epsilon}_t$  (%) = 0.38 is evaluated using Eq. (35)

The number of cycles to failure  $N_f$  used for fatigue damage calculation is estimated using the.

Eq. (9.3) in R66 [17] corresponding to type 316 weld metal. Using this data and Eq. (22), the fatigue damage is calculated.

•  $d_f = 1.6E-05$ 

Creep damage  $d_c$  and the total damage are calculated using equations (29) and (31).

- $d_c = 1.26E-03$
- $D = d_f + d_c = 0.001279$

Considering Fig. 4b corresponding to the crack initiation envelope, the allowable

creep-fatigue cycles before crack initiation are **782 cycles** for a dwell time of 300 h. Table 3 summarizes the allowable creep-fatigue cycles for 316L–316L at 550  $^{\circ}$ C. The weld assessment using RCC-MRx is more conservative than the weld assessment done using R5.

In addition to the previously identified sources of conservatism such as.

- · material properties variations
- the introduction of safety margins [22] in the RCC-MRx in fatigue curves which has a large contribution to the difference
- the fatigue damage assessment in R5 is based on crack nucleation and can be adapted to account for defect initiation of a specific size.
   RCC-MRx uses the endurance curves corresponding to a relatively large crack size
- RCC-MRx explicitly incorporates creep time into strain calculations, whereas R5 relies on ductility and stress relaxation data [22]. This means that when the dwell time is high, the creep strain also increases, which directly impacts the allowable creep-fatigue cycles. Additionally, the stress input to creep rupture curves differs between the two approaches [23].

the difference between the allowable creep-fatigue cycles obtained using the two codes can be justified by the following.

- the approach in R5 takes into account the weld geometry (weld cap angle) and its treatment (dressed or undressed). These aspects are not considered in RCC-MRx. Here, a dressed weld was considered for the R5 assessment like RCC-MRx.
- In the case of undressed and the presence of weld cap angle, the applied stress is enhanced using the SCF which can have a direct impact on the allowable cycles.

#### 3.4.3. Study case 3:316L welded to 10CrMo9-10

Previous sections highlighted that RCC-MRx is more conservative than R5 for both parent and welded materials. This section applies RCC-MRx to EBW dissimilar metal welds as a study case. Currently, in RCC-MRx [11] there are no rules dedicated to the creep-fatigue assessment on such types of EBW dissimilar metal welds considering the impact of the welding on the modification of materials properties especially in the case of dissimilar metals. The introduction of such weldments in the RCC-MRx creep-fatigue assessment is in progress.

# a) RCC-MRx assessment

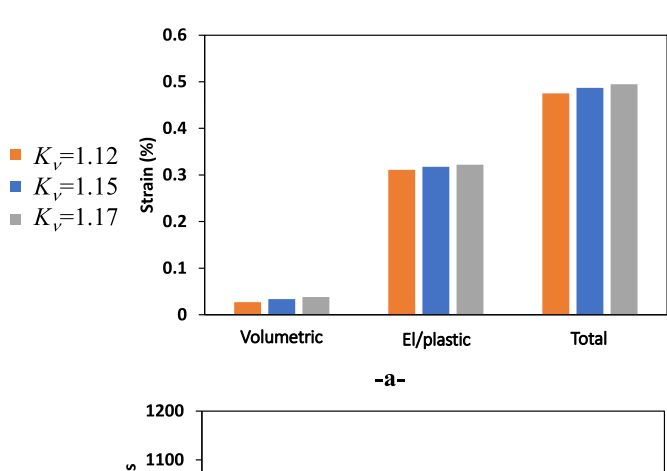
Figs. 14 and 15 represent the creep and fatigue curves available in RCC-MRx for 316L and 10CrMo9-10. According to these figures, the estimated creep life for the same creep rupture stress is lower for 10CrMo9-10, reinforcing the conservative selection of 10CrMo9-10 for creep-fatigue assessment, and so 10CrMo9-10 behaviour dictates the service life of this weldment (full penetration, Type I.1) under total stress range of 400 MPa.

Considering 10CrMo9-10 alone, using creep curves (Table A3.14AS.53 in Ref. [11]), the allowable creep hours are  $11.59\ h$ . As specific data related to the 10CrMo9-10 welds is unavailable in the RCC-MRx, the welding parameters given in A9.J3S, related to 316L, were used. The estimated allowable creep hours in the weld are  $8\ h$ .

Using fatigue curves (Table A3.14AS.47 in Ref. [11]) and the total strain calculated using the available data in A3.14AS (related to 10CrMo9-10) and A3.16AS (related to 2 ½ Cr1Mo in the absence of appropriate cyclic data for 10CrMo9-10), allowable fatigue cycles were estimated. The creep strain used for fatigue assessment was calculated using the creep law of 316L (A3.54 [11]) as this law is not available in Ref. [11] for 10CrMo9-10. Table 4 provides allowable cycles for various combinations of creep and fatigue, obtained using Fig. 4a.

From the comparison between the life assessment of 316L parent and 316 similar welded material, the selected weld factors applied have a significant impact on the results. This impact is particularly noteworthy as it significantly diminishes the permissible cycle count. For an identical dwell time of 300 h, the allowable cycles decrease significantly from 240 cycles for the 316L parent material to 100 cycles for the welded sample. In the context of dissimilar welds, beyond the influence of selected weld factors, the careful selection of the weakest material is crucial, as it dictates the service life. Notably, in the case of 10CrMo9-10, despite having a higher  $S_m$  than 316L at 550 °C, its creep-fatigue resistance properties are comparatively weaker than 316L, and so the failure is predicted in 10CrMo9-10. Therefore, the material selection process must be executed judiciously, considering not only the thermophysical properties but also the specific creep-fatigue resistance characteristics.

#### b) Experimental validation



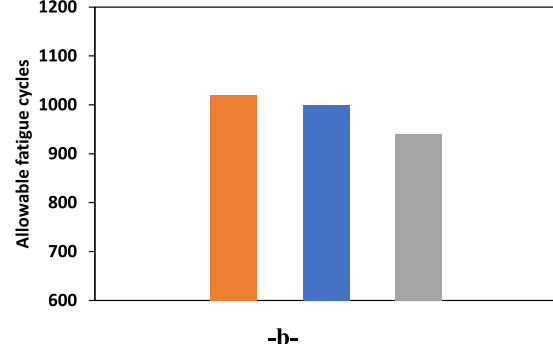


Fig. 13. Impact of the  $K_{\nu}$  variation on the strain values (-a-) and the allowable fatigue cycles (-b-).

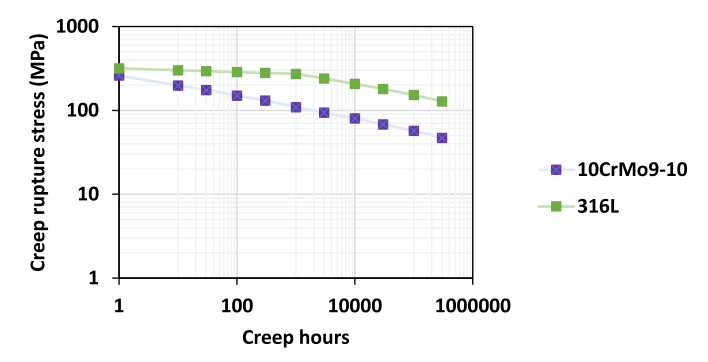


Fig. 14. Lower bound allowable creep rupture stress range values vs creep hours at 550 °C from RCC-MRx [11].

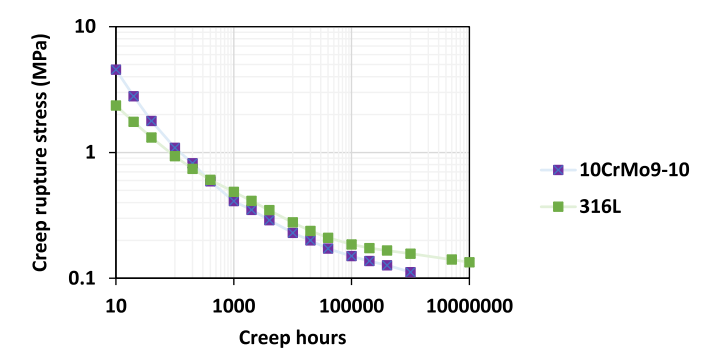


Fig. 15. Lower bound allowable fatigue strain range values vs numbers of fatigue cycles at 550 °C from RCC-MRx [11].

Table 4
Creep-fatigue assessment of 316L joined to 10CrMo9-10 using RCC-MRx.

Dwell time (hours)	Creep usage fraction W	Allowable cycles	Fatigue usage fraction V
2	0.25	320	0.42
3	0.38	175	0.26
5	0.63	90	0.15
7	0.88	25	0.04
7.5	0.94	18	0.03

316L plate was welded to 10CrMo9-10 using an autogenous EBW technique (I = 200 mA; E = 80 kV; speed = 6 mm/s; working distance = 560 mm) at NAMRC [24].

The crystallographic orientation evolution in the transition zones can have a direct impact on the welded material's mechanical properties, the reason why the evolution of crystallographic orientation has been conducted and represented in EBSD maps at different locations across the weld and the base metals, indicated as positions (a) through (g) in Fig. 16. Each map visualizes the grain orientations and structures, with colors corresponding to specific crystallographic orientations, as indicated in the color legend below (see Fig. 16).

**10CrMo9-10 parent** (Fig. 16a–c): The maps show uniform equiaxed grain structures. This homogeneity suggests minimal microstructural disturbance and uniform grain orientation distribution.

Fusion zone and Heat-Affected Zone (HAZ) of 10CrMo9-10 (Fig. 16d and e): The regions within the HAZ and the fusion zone show significant grain elongation and deformation and possible recrystallization effects, as evidenced by the irregular and varied grain structures. These microstructural changes are characteristic of the thermal effect induced during welding, leading to modifications in grain size and orientation.

Fusion zone and Heat-Affected Zone (HAZ) of 316L (Fig. 16f): This region, bridging the fusion zone and the 316L stainless steel,

exhibits a distinct mix of microstructures previously represented in Fig. 16g-h-i. The transition zone reflects differences in grain morphology and orientation, likely driven by differences in thermal conductivity and expansion between the two materials.

**316L Stainless Steel parent** (Fig. 16g): The 316L stainless steel region maintains a refined and relatively uniform grain structure. The stability of this microstructure under the influence of EBW highlights its thermal resilience compared to the more pronounced microstructural changes observed in 10CrMo9-10 steel.

Creep-fatigue samples were extracted from the EBW plates as represented Fig. 17a.

A strain-controlled creep-fatigue test [25] was conducted considering demanding creep conditions (11 h dwell time) to determine the number of cycles needed before sample failure. The applied strain was calculated using Eq. (7) and was 0.42 %. At these conditions, the sample is expected to fail within the first cycle. Two samples were tested and the axial strain was measured using two capacitive extensometers, with a 13 mm spacing between them, thus including the welding zone. The hysteresis creep-fatigue curves are represented in Fig. 18.

Both EBW samples exhibit reproducible cyclic stress-strain responses characterized by stress relaxation during the dwell time. Both hysteresis loops underline the cyclic plastic deformation, with the area enclosed by the loops representing the energy dissipated during each loading cycle. This indicates consistent material properties and behaviour due to the autogenous EBW process. In Fig. 18, sample 1 (19 cycles) and sample 2 (4 cycles) exhibit a reduction in yield strength in compression compared to tension, demonstrating the Bauschinger effect [26,27]. This effect is mainly visible in sample 1 and characterized by a lower yield stress in the opposite loading direction after the material has been pre-strained and so the asymmetry of the hysteresis loops, where the compressive stress at yield (during unloading/reverse loading) is lower than the initial tensile yield stress. This is due to the internal stress and microstructural changes caused by the prior plastic deformation in the opposite direction.

According to RCC-MRx calculations, the allowable creep hours in the weld are 8 h. Consequently, the samples were expected to fail within the first cycles. However, despite conducting 19 cycles (sample 1) and 4 cycles (sample 2), the samples did not fail. This can be justified by the following.

- selecting 10CrMo9-10 for the creep-fatigue assessment using RCC-MRx as the weakest material in terms of creep and fatigue resistance (Fig. 14 and Fig. 15) is very conservative and may not be representative of the autogenous EBW whose properties might be closer to 316L than to 10CrMo9-10. From the oxidized surface represented in Fig. 17b, it is noticed that the weld zone combines both materials due to diffusion. The oxidation occurs in the ferritic 10CrMo9-10 steel. The oxide scale thickness increases as a function of temperature and time [28]. The sample represented in Fig. 17b was tested at 550 °C.
- the experimental test is strain-controlled and hence the stress relaxes and a limited strain can accumulate. Consequently, the time spent at high stress during dwell is brief, resulting in minimal accumulated creep strain and reduced time under high stress. No creep strain data are available for 10CrMo9-10.
- the creep and fatigue data selected correspond to the lower bound allowable creep rupture stress and the lower bound allowable fatigue strain range which are used for the design rules and so are conservative in comparison with the average values.

#### 4. Conclusion

This paper presents a comparative analysis of two assessment procedures, R5 and RCC-MRx, utilized for ensuring the safe and reliable design of specific components in fusion applications, with a focus on DEMO components currently in development. It offers an overview of

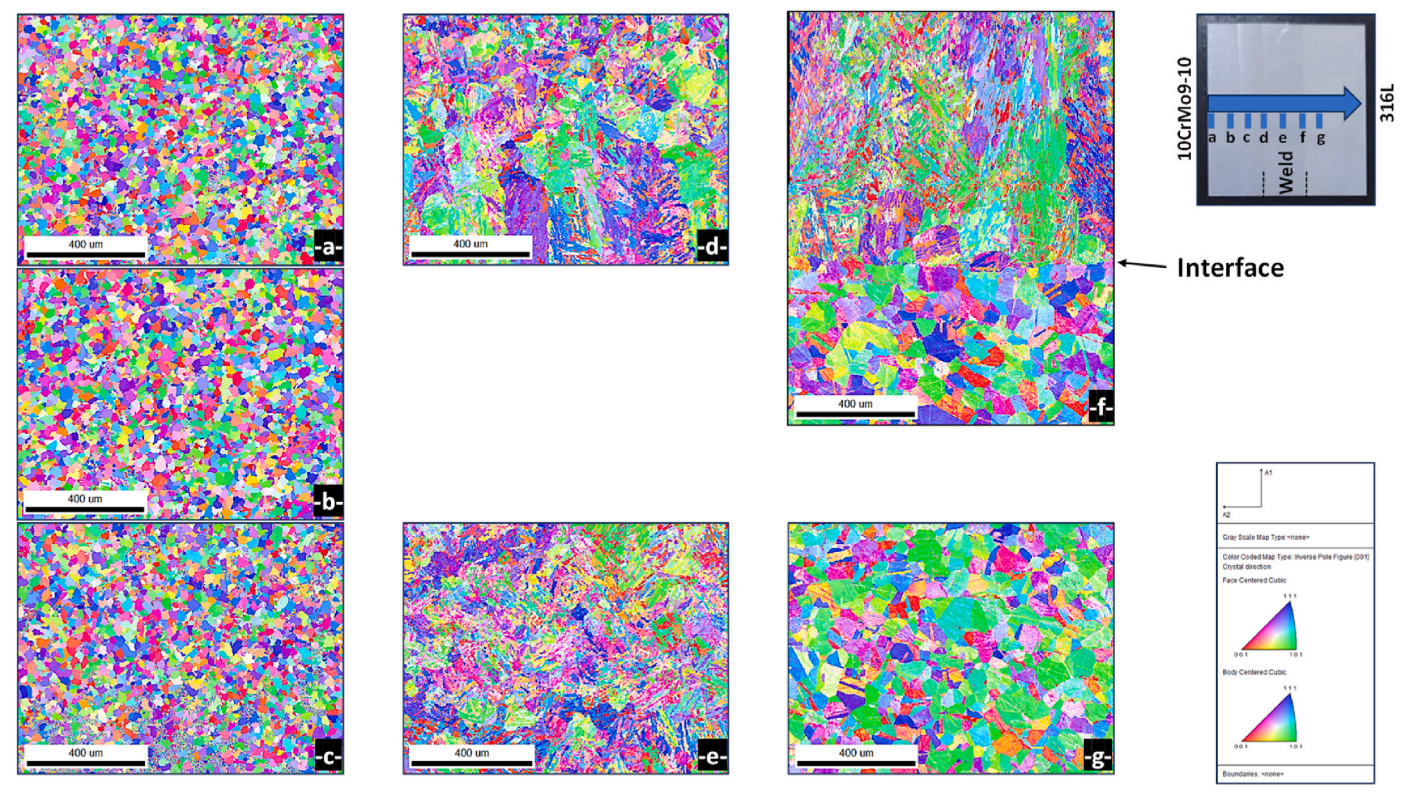


Fig. 16. Crystallographic orientation maps of the weld and the parent dissimilar metals obtained by EBSD analysis across positions (a) to (g).

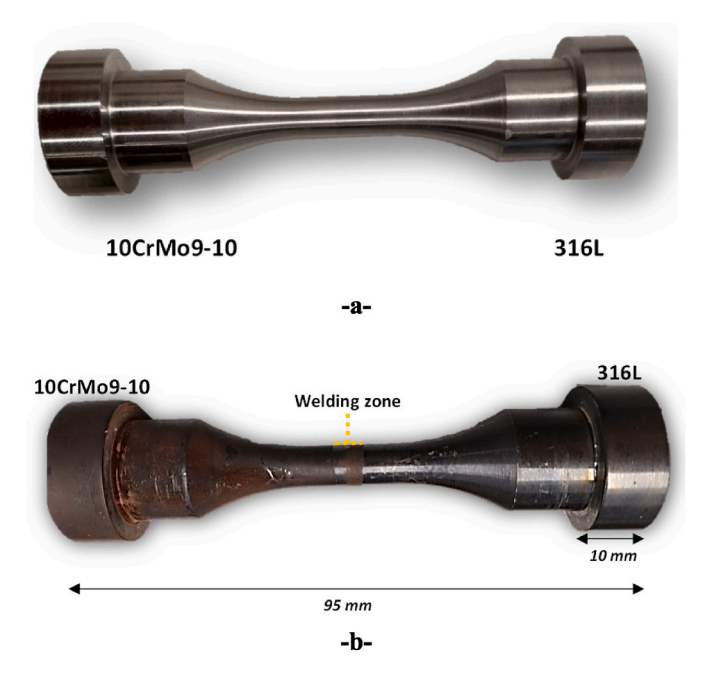


Fig. 17. Creep-fatigue sample before (-a-) and after (-b-) testing.

the creep-fatigue assessment methods of R5 (detailed and simplified approaches) and RCC-MRx, highlighting their differences and similarities. The comparison is initiated by analyzing the material properties of 316L under conditions identical to those used in R5 and RCC-MRx, exploring the impact of varying factors on the assessment, and comparing the calculated total strain required for creep-fatigue assessment of each procedure for 316L at  $550^{\circ}\text{C}$ . Results indicate that RCC-MRx exhibits greater conservatism under these conditions. The main

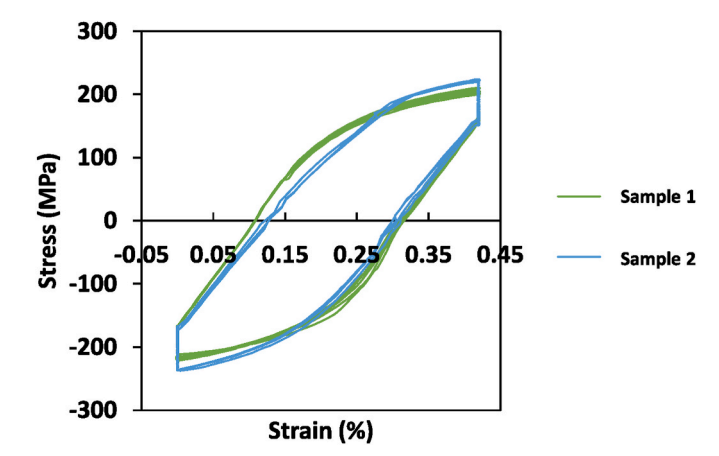


Fig. 18. Experimental hysteresis curve for 316L to 10CrMo9-10 DMW.

observed sources of conservatism are.

- the differences in material properties in R66 used for R5 assessment and those in RCC-MRx for the same materials at the same conditions in addition to the safety margins included in RCC-MRx.
- the calculation of the fatigue damage per cycle is related to crack nucleation and can be adjusted to account for the initiation of a defect of a given size, whereas the RCC-MRx uses the endurance curves defined from a specific load drop which can correspond to a relatively large crack size.

Furthermore, a creep-fatigue life assessment, including weld assessment approaches, was conducted for 316L and similar metal welds (316L-to-316L) using R5 and RCC-MRx. The difference between the allowable creep-fatigue cycles obtained using the two procedures can be attributed to the above sources of conservatism in RCC-MRx. Besides,

although they weren't considered here, the residual stresses are considered in the weld R5 assessment and may also have a direct impact on the allowable cycles.

#### CRediT authorship contribution statement

Younes Belrhiti: Writing – review & editing, Writing – original draft, Visualization, Methodology, Investigation, Conceptualization. Cory Hamelin: Writing – review & editing, Supervision, Funding acquisition, Conceptualization. Pierre Lamagnère: Writing – review & editing, Supervision, Methodology. Mahmoud Mostafavi: Writing – review & editing, Supervision, Funding acquisition, Conceptualization.

#### Declaration of competing interest

The authors declare the following financial interests/personal relationships which may be considered as potential competing interests: Cory Hamelin reports financial support was provided by Engineering and Physical Sciences Research Council. Mahmoud Mostafavi reports financial support was provided by Royal Academy of Engineering. If there are other authors, they declare that they have no known competing financial interests or personal relationships that could have appeared to influence the work reported in this paper.

#### Acknowledgements

This work has been part-funded by the EPSRC Energy Programme, grant number EP/W006839/1, and RAEng Fellowship grant number RCSRF1920\9\46.

To obtain further information on the data and models underlying this paper please contact PublicationsManager@ukaea.uk\*.

The authors would like to express their gratitude to.

- EDF Energy Nuclear Generation Ltd. for authorizing the use of R5 and R66 for this work
- RCC-MRx Sub-Committee Chairwoman Cécile Petesch and Dr Yves Lejeail (CEA) for their valuable feedback
- Dr Thomas Dutilleul (NAMRC) for EBW joining of the plates

#### Data availability

Data will be made available on request.

#### References

[1] M. Messner, B. Barua, A. Rovinelli, T. Sham, Environmental creep-fatigue and weld creep cracking: a summary of design and fitness-for-service practices, Argonne

- National LaboratoryANL-19/13, Jan. 2020. Report prepared for the U.S. Nuclear Regulatory Commission.
- [2] M.T. Yavuz, I. Ozkol, Thermal structural design aspects of military aircraft, Journal of Aeronautics and Space Technologies 17 (1) (Jan. 2024) 1.
- [3] R. Viswanathan, et al., U.S. program on materials technology for ultra-supercritical coal power plants, J. of Materi Eng and Perform 14 (3) (Jun. 2005) 281–292.
- [4] R. Viswanathan, J. Stringer, Failure mechanisms of high temperature components in power plants, J. Eng. Mater. Technol. 122 (3) (Jul. 2000) 246–255.
- [5] P. Frosi, G. Mazzone, J.-H. You, Structural design of DEMO Divertor Cassette Body: provisional FEM analysis and introductive application of RCC-MRx design rules, Fusion Eng. Des. 109–111 (Nov. 2016) 47–51.
- [6] M. Muscat, P. Mollicone, J.H. You, N. Mantel, M. Jetter, Creep fatigue analysis of DEMO divertor components following the RCC-MRx design code, Fusion Eng. Des. 188 (Mar. 2023) 113426.
- [7] M.E. Kassner, T.A. Hayes, Creep cavitation in metals, Int. J. Plast. 19 (10) (Oct. 2003) 1715–1748.
- [8] P. Rodriguez, K. Bhanu Sankara Rao, Nucleation and growth of cracks and cavities under creep-fatigue interaction, Prog. Mater. Sci. 37 (5) (Jan. 1993) 403–480.
- [9] M. Sauzay, M. Mottot, L. Allais, M. Noblecourt, I. Monnet, J. Périnet, Creep-fatigue behaviour of an AISI stainless steel at 550 °C, Nucl. Eng. Des. 232 (3) (Aug. 2004) 219–236.
- [10] EDF Energy, "Assessment procedure R5 2/3 (3) (2014).
- [11] AFCEN, Design and Construction Rules for Mechanical Components of Nuclear Installations: High Temperature, Research and Fusion Reactors, RCC MRx, 2018.
- [12] D. De Meis, RCC-MRx Design Code for Nuclear Components, 2015.
- [13] BPVC | 2023 Boiler and Pressure Vessel Code ASME".
- [14] E. Vacchieri, Review: creep-fatigue interaction testing and damage assessment for high temperature materials, in: Reference Module in Materials Science and Materials Engineering, Elsevier, 2016.
- [15] Y. Belrhiti, C. Hamelin, D. Knowles, M. Mostafavi, Life Assessment of Metals Used in Fusion Using R5 and RCC-MRx, 2024.
- [16] P. Lamagnère, et al., Design rules for ratcheting damage in AFCEN RCC-MRX 2012 code. Presented at the ASME 2014 Pressure Vessels and Piping Conference, American Society of Mechanical Engineers Digital Collection, Nov. 2014.
- [17] E.D.F. Energy, AGR Materials Data Handbook R66 Revision 10, 2016.
- [18] D.M. Knowles, R5 high temperature creep-fatigue life assessment for austenitic weldments, Procedia Eng. 86 (2014) 315–326.
- [19] E.W. Horton, et al., The inclusion and role of micro mechanical residual stress on deformation of stainless steel type 316L at grain level, Materials Science and Engineering: A 876 (Jun. 2023) 145096.
- [20] H.-Y. Lee, Comparison of elevated temperature design codes of ASME Subsection NH and RCC-MRx, Nucl. Eng. Des. 308 (Nov. 2016) 142–153.
- [21] E.D.F. Energy, NNL, Rolls-Royce and BEIS, Guidance for the structural integrity demonstration of advanced modular reactors in the UK, 2022. Report number: EASICS/001.
- [22] P. James, P. Lamagnère, Y. Lejeail, T. Lebarbé, C. Petesch, S. May, RCC-MRx and R5 Creep-Fatigue Initiation Predictions Applied to the EVASION Tests, Jul. 2022.
- [23] P. James, D. Coon, C. Austin, N. Underwood, M. Chevalier, D. Dean, Overview of EASICS validation experiments and code comparison of R5, RCC-MRX and ASME III division V. Presented at the ASME 2020 Pressure Vessels & Piping Conference, American Society of Mechanical Engineers Digital Collection, Oct. 2020, https:// doi.org/10.1115/PVP2020-21720.
- [24] B. Baufeld, T. Dutilleul, Electron Beam welding of large components for the nuclear industry, MATEC Web Conf. 269 (2019) 02009.
- [25] Y. Belrhiti, C. Hamelin, D. Knowles, M. Mostafavi, Thermomechanical analysis of tungsten-copper joints for fusion applications using digital image correlation, Fusion Eng. Des. 206 (Sep. 2024) 114608.
- [26] R. Sowerby, D.K. Uko, Y. Tomita, A review of certain aspects of the Bauschinger effect in metals, Mater. Sci. Eng. 41 (1) (Nov. 1979) 43–58.
- [27] P.S. Bate, D.V. Wilson, Analysis of the bauschinger effect, Acta Metall. 34 (6) (Jun. 1986) 1097–1105.
- [28] J. Lehmusto, D. Lindberg, P. Yrjas, L. Hupa, The effect of temperature on the formation of oxide scales regarding commercial superheater steels, Oxid Met 89 (1) (Feb. 2018) 251–278.